An ensemble estimate of Australian soil organic carbon using machine learning and process-based modelling

Lingfei Wang[1,2], Gab Abramowitz[1,2], Ying-Ping Wang[3], Andy Pitman[1,2] and Raphael A. Viscarra Rossel[4]

[1] ARC Center of Excellence for Climate Extremes, Sydney NSW 2052, Australia
[2] Climate Change Research Center, University of New South Wales, Sydney NSW 2052, Australia
[3] CSIRO Environment, Private Bag 10, Clayton South VIC 3169, Australia
[4] Soil & Landscape Science, School of Molecular & Life Sciences, Faculty of Science & Engineering, Curtin University, GPO Box U1987, Perth WA 6845, Australia.

Correspondence to: Lingfei Wang (lingfei.wang@unsw.edu.au)

Abstract

Spatially explicit prediction of soil organic carbon (SOC) serves as a crucial foundation for effective land management strategies aimed at mitigating soil degradation and assessing carbon sequestration potential. Here, using more than 1000 in-situ observations, we trained two machine learning models (random forest, and K-means coupled with multiple linear regression), and one process-based model (the vertically resolved MIcrobial-MIneral Carbon Stabilization (MIMICS)) to predict SOC stocks of the top 30 cm of soil in Australia. Parameters of MIMICS were optimized for different site groupings, using two distinct approaches, plant functional types (MIMICS-PFT), and the most influential environmental factors (MIMICS-ENV). All models showed good performance in SOC predictions with R^2 greater than 0.8 during out-of-sample validation with random forest being the most accurate, and SOC in forests is more predictable than that in non-forest soils excluding croplands. The performance of continental-scale SOC predictions by MIMICS-ENV is better than that by MIMICS-PFT especially in non-forest soils. Digital maps of terrestrial SOC stocks generated using all the models showed similar spatial distribution with higher values in southeast and southwest Australia, but the magnitude of estimated SOC stocks varied. The mean ensemble estimate of SOC stocks was 30.3 t ha^{-1} with K-means coupled with multiple linear regression generating the highest estimate (mean SOC stocks at 38.15 t ha^{-1}) and MIMICS-PFT generating the lowest estimate (mean SOC stocks at 24.29 t ha^{-1}). We suggest that enhancing process-based models to incorporate newly identified drivers that significantly influence SOC variations in different environments could be key to reducing the discrepancies in these estimates. Our findings underscore the considerable uncertainty in SOC estimates derived from different modelling approaches and emphasize the importance of rigorous out-of-sample validation before applying any one approach in Australia.

1. Introduction

Globally, the soil is the largest biogeochemically active terrestrial carbon pool, storing more organic carbon than plants and the atmosphere combined (Jackson et al., 2017). The turnover of soil organic carbon (SOC) is a key function in plant growth, maintenance of soil water and nutrients, soil structure stabilization and other biogeochemical processes (Lefèvre et al., 2017). Soil can act as either a carbon sink or carbon source depending on the balance of carbon input through plant litter and root exudates and output through respiration and leaching (Terrer et al., 2021; Panchal et al., 2022). Even a small change in SOC stocks, in any direction, could significantly affect the atmospheric concentration of CO_2 and thereby climate change (Stockmann et al., 2013).

Given the importance of SOC, there is now a large and growing interest in estimating spatially explicit SOC content and stocks. SOC supports critically important soil-derived ecosystem services, and the amount of SOC indicates the degree of land and soil degradation (Lorenz et al., 2019). SOC content below a certain limit will lead to the decline of microbial diversity, water holding capacity and soil productivity (Stockmann et al., 2015). Additionally, with growing concerns about increasing anthropogenic CO_2 emissions, soil carbon sequestration has emerged as a potential strategy for climate change mitigation (Smith, 2016; Rumpel et al., 2018). Protection of existing SOC and rebuilding depleted stocks through land management are potential strategies in mitigating climate change (Bossio et al., 2020). However, effective SOC management requires accurate knowledge of its existing distribution. Reliable estimates of SOC stocks and their spatial variation serve as a reference point for assessing how close soil is to its maximum SOC storage capacity and its potential to sequester additional carbon (Six et al., 2002; Georgiou et al., 2022). Precise estimation of contemporary SOC stocks also provides a baseline map that can be used to calibrate and initialize dynamic-mechanistic models, enabling the study of how SOC will respond to climate and land-use change (Minasny et al., 2013; Viscarra Rossel et al., 2014). It is, for example, a prerequisite for accurately predicting future carbon–climate feedback in Earth system models (ESMs) (Todd-Brown et al., 2013).

Accurately assessing SOC storage is challenging due to the complexity of carbon formation and degradation processes in space and time (Keskin et al., 2019). Soil exists as a continuum containing organic compounds at different stages of decomposition (Lehmann and Kleber, 2015). Soil formation can be described by a function of climate, organisms, relief, parent material and time (Jenny, 1941). These factors are widely used in SOC studies for digital soil mapping (McBratney et al., 2003; Viscarra Rossel et al., 2015; Liang et al., 2019). However, the relationship between SOC storage and these driving variables is complex and spatially variable (Mishra and Riley, 2015; Viscarra Rossel et al., 2019; Adhikari et al., 2020) leading to substantial challenges and inherent uncertainties in SOC predictions.

Mechanistic process-based models and empirical models (including machine learning models) are two widely employed approaches used to predict SOC stocks and their spatial distribution.

Conventional process-based models assume first-order kinetics for SOC decomposition, wherein the rate of C decomposition is dependent on temperature and moisture but independent of microbial biomass, and equilibrium SOC stock is proportional to carbon input and mean residence time (Abs and Ferrière, 2020; Wang et al., 2021). ESMs coupled with conventional SOC models cannot accurately simulate spatial pattern of contemporary soil carbon and show large divergence in projected SOC dynamics under future climate change (Todd-Brown et al., 2013; Todd-Brown et al., 2014). In addition to the biases introduced by errors in model parameters and the lack of independent model validation based on observed time series data, the uncertainties in predicted SOC by ESMs can also result from the lack of explicit representation of soil microbial activities and metabolic traits (Wieder et al., 2015; Le Neo et al., 2023). Numerous microbial models have been developed in the past few decades to improve model performance of SOC predictions (Chandel et al., 2023), but these models have rarely been incorporated into large-scale modelling frameworks due to the difficulty of constraining parameters relating to microbial activities and the lack of rigorous validation (Todd-Brown et al., 2013; Luo et al., 2016). Process-based SOC models are constructed based on our understanding of the major processes governing SOC dynamics (e.g., carbon input, decomposition, and loss). However, the disagreement in projections of carbon dynamics by different models highlights the need to improve our knowledge of SOC cycling (Luo et al., 2016). Machine learning models without any process-level assumptions provide a tool to identify the most influential controls on SOC variations. Machine learning models can represent non-linear and non-smooth relationships between predictor and response variables as well as interactions between different predictors (Heung et al., 2016). Various machine learning algorithms have been successfully used in digital soil mapping to predict high-resolution spatially explicit SOC concentration/stocks (Lamichhane et al., 2019).

Several modelling studies of soil carbon stocks have been conducted in Australia. Wang et al. (2018a) trained boosted regression trees and random forest models using field observations and applied the trained random forest model to map the spatial distribution of SOC at two soil depths (0-5 cm and 0-30 cm) for the semi-arid rangelands of eastern Australia. Continentally, Viscarra Rossel et al. (2014) trained the CUBIST model, a form of piecewise linear decision tree, using more than five thousand observations to produce a high resolution (90 m × 90 m) baseline map of SOC stocks of Australian terrestrial systems and its uncertainty of the top 30 cm soils. Based on the baseline map, Walden et al. (2023) derived spatially explicit estimates of Australian SOC stocks and uncertainty including additional data from forests from southeastern Australia and coastal marine (or blue carbon) ecosystems. SOC content at multiple soil depths along with associated uncertainties were also estimated using different machine learning algorithms (Viscarra Rossel et al., 2015; Wadoux et al., 2023). Moreover, the distribution of different soil carbon compositions (i.e., the particulate, mineral-associated and pyrogenic organic carbon fractions) and the importance of environmental factors on their variations were also studied using machine learning (Viscarra Rossel et al., 2019). However, despite the progress made in SOC modelling, significant uncertainties persist in SOC estimates due to the inherent complexities of SOC variations and the lack of appropriately sampled SOC observations. All

these continental estimates were generated using empirical modelling approaches or first-order biogeochemical models without explicitly representing the important role of soil microbes in SOC stabilization (Grace et al., 2006; Lee et al., 2021). Estimates from mechanistic SOC models with explicit representation of microbial metabolism are missing despite offering the potential to better constrain SOC dynamics under future climate change scenarios in a way that empirical approaches cannot.

Our primary objective in this paper is to assess the predictability of SOC concentration (excluding cropland soils) in Australia and generate a range of estimates of terrestrial SOC stocks, employing both process-based and empirical modelling, and examine why these estimates might differ. First, we discern the significance of environmental predictors, both at continental and biome scales. We then evaluate the performance of random forests, K-means with multiple linear regression and the vertically resolved MIMICS model with different parametrization approaches. Finally, we compare the spatial estimates of SOC stocks using these different approaches across Australia, and discuss their differences and potential application to future SOC projection.

2. Materials and Methods

2.1. Model descriptions

2.1.1. Vertically resolved MIMICS

The MIMICS model (Wieder et al., 2015; Zhang et al., 2020) explicitly considers relationships between litter quality, functional trade-offs in microbial physiology, and the physical protection of microbial by-products in forming stable soil organic matter. There are two litter pools: metabolic (LIT_m) and structural (LIT_s) litter (Figure 1), and the partitioning of litter input into metabolic and structural pools is determined by the chemical properties of the litter. Litter and SOC turnover are governed by two microbial functional types that exhibit copiotrophic (i.e., r-selected, MIC_r) and oligotrophic (i.e., K-selected, MIC_k) growth strategies. The MIC_r is assumed to have higher growth and turnover rates, and a preference for consuming labile litter (LIT_m), while MIC_k is characterized by lower growth and turnover rates, and a greater competitive advantage when consuming low-quality litter (LIT_s) and chemically recalcitrant SOC. SOC in MIMICS is divided into three pools: physically protected (SOC_p), (bio)chemically recalcitrant (SOC_c) and available (SOC_a) carbon (Figure 1).

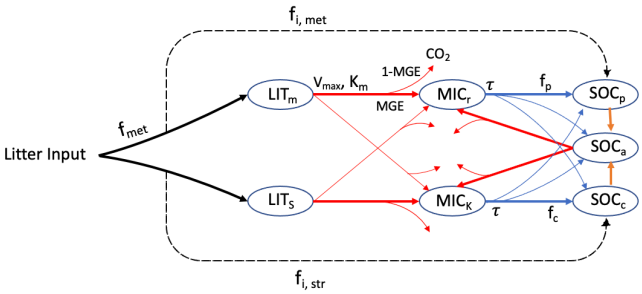

Figure 1. SOC pools and fluxes represented in MIMICS (adapted from Wieder et al., (2015)). Litter inputs are partitioned into metabolic and structural litter pools (LIT_m and LIT_s) based on litter quality (f_{met}). Decomposition of litter and available SOC pool (SOC_a) are governed by temperature sensitive Michaelis-Menten kinetics (V_{max} (maximum reaction velocity) and K_m (half saturation constant)), shown by red lines. Microbial growth efficiency (MGE) determines the partitioning of C fluxes entering microbial biomass pools vs. heterotrophic respiration. Turnover of microbial biomass (τ, blue) depends on microbial functional types (MIC_r and MIC_k), and is partitioned into available, physically protected and chemically recalcitrant SOC pools (SOC_a, SOC_p and SOC_c, respectively).

The decomposition of litter pools and SOC pools follows temperature-sensitive Michaelis-Menten kinetics. Microbial growth efficiency (MGE) determines the partitioning of carbon fluxes entering microbial biomass pools (MIC_r and MIC_k) versus heterotrophic respiration. Access of microbial enzymes to available substrates depends on soil texture. The equations of MIMCS are from Wieder et al. (2015), except that the density-dependent microbial turnover was introduced to MIMCS to minimize an unrealistic oscillation (Zhang et al., 2020). To better simulate carbon turnover at different soil depths, vertical transport of soil carbon was introduced into MIMICS considering carbon transported through bioturbation and diffusion among adjacent soil layers (Wang et al., 2021).

Vertically resolved MIMICS is run using a daily time step. The soil was divided into 15 layers, each of 10 cm thickness. All the sites in this study are assumed to be at steady state (i.e., no interannual variation of SOC). Historical climate, litterfall input and soil properties were all assumed to be similar to the average conditions. At each site, the initial pool fractions were 0.03, 0.03, 0.14, 0.47 and 0.33 for MIC_r, MIC_k, SOC_p, SOC_c and SOC_a, respectively. All pools were then spun up to finally achieve steady state with the maximal difference in any pool size between two successive spins being less than 0.05%.

2.1.2. Machine learning

Two machine learning algorithms were applied in this study to predict SOC. First, random forest (RF) is a tree-based ensemble learning method that works by building a set of regression trees and averaging results (Breiman, 2001). Within the training procedure, the RF algorithm produces multiple trees. Each regression tree in the forest is independently constructed based on a unique bootstrap sample (with replacement) from the original training data set. The

response, as well as the predictor variables are either categorical (classification trees) or numeric (regression trees). Bootstrap sampling makes RF less sensitive to overfitting and allows for robust error estimation based on the remaining test set, the so-called Out-Of-Bag (OOB) sample (Wiesmeier et al., 2014). We used the "ranger" package R (version 4.2.0) for RF computation. We trained the RF model with different numbers (100, 200, 300, 400 and 500) of trees and observed that the model's performance remained similar regardless of the number of trees used. The number of regression trees generated in the forest (num.trees) was finally set as 200, and the number of predictors randomly selected at each node (mtry) was set as default, which was 2.

Multiple linear regression (MLR) is widely used in SOC studies but found to be less effective than machine learning algorithms (Lamichhane et al., 2019). Here, instead of applying MLR directly with all environmental factors as predictors, our approach involved a preliminary step where we partitioned all observations into distinct clusters using K-means, an unsupervised machine learning algorithm. K-means aims to divide the data into a predefined number of clusters (k), with the objective of maximizing the similarity among data within each cluster. The underlying assumption here was that sites sharing similar environmental conditions would exhibit comparable SOC concentration. In cases where certain clusters had fewer observations than five times the number of predictors, we augmented these clusters by incorporating observations from other clusters. This augmentation process was guided by the Euclidean distance between the observation and the cluster centre, ensuring a more robust construction of the linear regression model. To determine the number of clusters, we applied the coupled K-means and MLR with varying number of clusters. The selection of the optimal number of clusters was based on the criterion of producing the smallest root mean square error during independent out-of-sample validation.

2.2. Relative importance of environmental variables for SOC prediction

RF-based measures of variable importance have gained widespread popularity as tools for evaluating the contributions made by predictor variables within a fitted random forest model (Debeer and Strobl, 2020). In the context of this study, we employed permutation variable importance (PVI) within the random forest framework to gauge the significance of predictors (see Section 2.4) in predicting SOC concentration.

The PVI entails measuring the reduction in a RF model's performance score upon random shuffling of a single variable values. By doing so, the inherent relationship between the variable and the SOC concentration is disrupted. Consequently, the disparity in prediction accuracy observed in a RF model before and after such shuffling serves as a quantitative representation of the significance of the particular predictor in predicting SOC concentration. The greater the importance of the predictor, the higher its corresponding PVI value becomes.

2.3. Parameter optimization

MIMICS parameters were derived from Zhang et al. (2020) and Wang et al. (2021), except that five parameters (Table 1) which directly control the organic carbon decomposition were optimized. An effective global optimization algorithm called the shuffled complex evolution (SCE-UA, version 2.2) method (Duan et al., 1993) was applied for parameter optimization by minimizing the sum of squared residuals between the observed and modelled values.

Vertically resolved MIMICS simulated SOC concentration for 15 soil layers with a uniform layer thickness of 10 cm. As observations only provide one measurement for the top 30 cm soil, we computed the average of the modelled values spanning the 0-10 cm, 10-20 cm, and 20-30 cm soil layers. This average was then adopted as the modelled SOC concentration for top 30 cm soil, serving as the basis for evaluating the difference between observations and simulations.

Table 1. The optimized model parameters (dimensionless) and their value range.

Parameter	Definition	Range
a_v	A scaling factor for V_{max}	0-30
a_k	A scaling factor for K_m	0-20
xdesorp	A scaling factor for SOC desorption rate	0-3
xbeta	An exponent of the biomass density dependent mortality rate of microbes	1.05-2
xdiffsoc	A scaling factor for SOC diffusion coefficient in soil	0-30

Parameters in MIMICS were optimized for different groups divided based on two approaches. The first approach involved categorizing all observations into four groups based on plant functional type (PFT). The second approach used the most influential abiotic variables as predictors (as outlined in Section 2.2) and divided all observations into 6 clusters using the K-means algorithm. The determination of the optimal number of clusters was achieved through the minimization of the sum of the within-cluster-sum-of-squares-of-all-clusters (WCSSE), a process facilitated by the "ClusterR" package in R (version 4.2.0). This clustering aimed to ensure the highest possible similarity among the environmental factors within each cluster. It was anticipated that SOC ranges within each cluster would be narrow due to the high similarity of environmental predictors.

2.4. Data

2.4.1. Predictors of spatial variations of observed SOC concentration

MIMICS requires gridded mean annual temperature (MAT), carbon input and clay content as driving variables for a spatial simulation. Gridded mean annual precipitation (MAP) and vegetation types were also used during calibration and when understanding the drivers and spatial variability of SOC. Details of gridded data can be found in Table 2.

Gridded daily maximum temperature, minimum temperature, and precipitation at 0.05° resolution were obtained from the SILO database (Jeffrey et al., 2001) of Australian climate data. Mean daily temperature was approximated as the average of maximum and minimum

daily temperature. MAT was calculated from mean daily temperature from 1991 to 2020, and MAP was calculated from daily precipitation from 1991 to 2020.

Carbon input was represented by NPP. Gridded mean annual NPP at 500 m was calculated based on annual NPP from 2001 to 2020 obtained from MODIS (MOD17A3HGF V6.1) (Running and Zhao, 2021). NPP was partitioned to above-/belowground part by multiplying by the root/shoot ratio for different vegetation types (Mokany et al., 2006). Here we did not account for the faction of NPP that is appropriated by human activities.

The distribution of vegetation types at 3'' resolution was obtained from National Vegetation Information System (NVIS, version 6.0, https://www.dcceew.gov.au/environment/land/native-vegetation/national-vegetation-information-system). Pixels of non-vegetated regions were removed and 28 types from NVIS were aggregated to just 4 PFT: forest, woodland, shrubland and grassland.

Soil bulk density and clay content were obtained from Soil and Landscape Grid National Soil Attributes Maps (SLGA – Release 2) (Grundy et al., 2015; Viscarra Rossel et al., 2015). Soil properties were predicted based on machine learning at depths 0-5 cm, 5-15 cm, 15-30 cm, 30-60 cm, 60-100 cm, and 100-200 cm in SLGA. Bulk density and clay content were estimated for top 30 cm soil as weighted average of first 3 layers in SLGA.

The initial spatial resolution of the gridded data was maintained when extracting the required environmental factors for each SOC observation. All data were then resampled to 0.05° resolution using bilinear interpolation for estimation of terrestrial SOC stocks at continental scale.

Table 2. Information of gridded data used in this study.

	Source	Spatial Scale	Temporal Scale	Unit	Time Period
Maximum Temperature	SILO	~5 km	daily	°C	1991-2020
Minimum Temperature	SILO	~5 km	daily	°C	1991-2020
Precipitation	SILO	~5 km	daily	mm	1991-2020
NPP	MODIS	500 m	annually	g C/m^2/year	2001-2020
Vegetation Types	NVIS	100 m	/	/	/
Soil Bulk Density	SLGA	~90 m	/	kg/m^3	/
Soil Clay Content	SLGA	~90 m	/	%	/

2.4.2. Soil organic carbon observations

SOC observations for top 30 cm soil in Australia were collected from two datasets. The first dataset is described in Viscarra Rossel et al. (2014) and Viscarra Rossel et al. (2019). We removed the observations collected from croplands based on the land-use record in the dataset and removed those from unvegetated regions based on NVIS vegetation map (see above). A total of 1070 site observations with only 38 from forest soils were retained. SOC stocks were reported in t ha^{-1}. To better represent SOC distribution in forest, we obtained additional forest SOC observations from a second dataset, the Biomes of Australian Soil Environments (BASE)

described in Bissett et al. (2016). Here, SOC (%) was reported for 0-10 and 20-30 cm. We estimated SOC for 0-30 cm soil following the method described in Viscarra Rossel et al. (2014).

To compare the observations with MIMICS outputs, we then converted both simulated SOC (mg/cm^3) and observed SOC (t/ha) in the first dataset (Viscarra Rossel et al. 2014) to SOC concentration (g C/kg soil) using spatially explicit soil bulk density (BD) from SLGA. The unit conversion will not affect the results of MIMICS. Soil clay content is extracted from SLGA.

The spatial distribution of SOC observations from different PFT is shown in Figure 2a. SOC concentration in top 30 cm is positively skewed, ranging from 1.36 to 59.73 g C/kg soil with mean value at 9.97 g C/kg soil and median value at 6.11 g C/kg soil. SOC concentration in grassland, shrubland and woodland show similar distribution patterns (Figure 2b), while SOC concentration in forest is more variable with a standard deviation at 15.92 g C/kg soil.

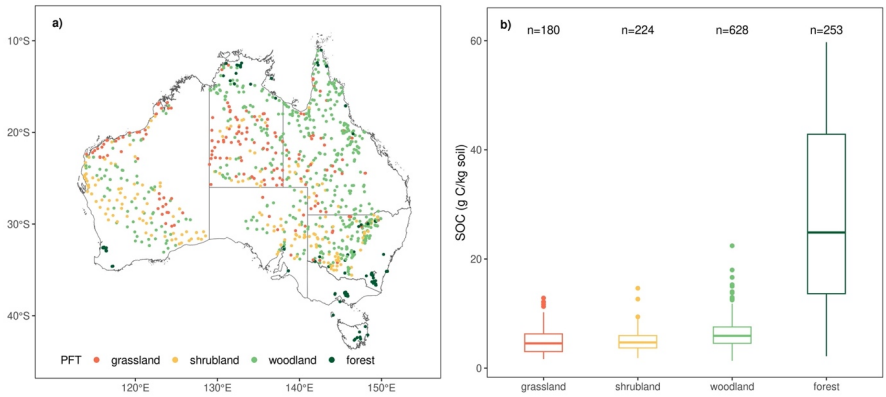

Figure 2. a) Spatial distribution of 1285 soil organic carbon observations used in this study and the plant functional types which they belong to; b) boxplots of SOC concentration distributions for each plant functional type. For boxplots, centre lines represent the median value, and upper and lower box boundaries represent third and first quartile. Whiskers extend to the smallest and largest values within 1.5 times the interquartile range.

2.5. Model evaluation

For machine learning models, 70% of the observations were randomly selected as training data to train the models and the remaining 30% used as test data to validate the predictions of SOC concentration. For vertically resolved MIMICS, parameters were optimized for each PFT or environmental group (see Section 2.3 above), and we again randomly selected 70% of

observations in each group to train the model and used the remaining 30% for validation. To cross-validate, the procedure was repeated 10 times.

The performance of models was evaluated using four metrics. Mean Absolute Error (MAE) indicates how close the average predictions are to average observations. Root Mean Square Error (RMSE) measures the overall accuracy combining mean, standard deviation differences (across sites) and (spatial) correlation. Coefficient of determination (R^2) measures the percentage of variation explained by the model. Lin's Concordance Correlation Coefficient (LCCC) (Lawrence and Lin, 1989) measures the level of agreement between predictions and observations following the 1:1 line. A good model will have MAE and RMSE close to 0 and R^2 and LCCC close to 1.

2.6. Estimation of terrestrial SOC stocks

SOC concentrations were used to train the models, and we then estimated terrestrial SOC stocks and their continental-scale spatial distribution in top 30 cm soil utilizing the four models validated within this study. SOC stock (t ha^{-1}) is calculated using SOC concentration (g C/kg soil), bulk density (BD, kg/m^3) and soil depth (m),

$$SOC_{stock} = SOC_{concentration} \times BD \times depth/100 \quad (2)$$

In the cases of MIMICS-PFT and MIMICS-ENV, the initial step involved grouping all pixels into four distinct plant functional groups or six environmental clusters. Since cross-validation was performed, the machine learning and process-based models were evaluated using test data, and the models with the optimal performance were subsequently employed at each pixel to estimate terrestrial SOC stocks. The map of ensemble estimate of SOC stocks was produced as the average of four model estimates at each pixel.

3. Results

3.1. Relative importance of environmental predictors of SOC concentration

Using the PVI in random forest, we identified the significance of environmental factors in predicting SOC concentration. At the continental scale, soil bulk density contributes most to the prediction of SOC concentration, following by MAT, NPP and MAP (Figure 3). Soil clay content and plant functional type exhibit relatively lesser significance in this regard.

The relative predictor importance for forests and grasslands aligns with the importance at continental scale. In shrubland and woodland, NPP and MAP emerge as the pivotal factors. Collectively, across both continental and regional scales, soil bulk density, MAT, and MAP are the three most influential abiotic factors.

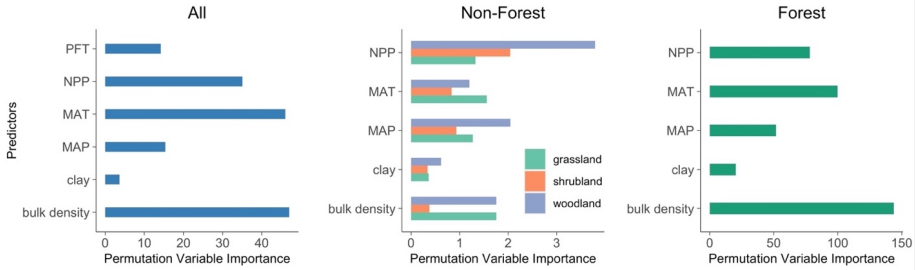

Figure 3. Importance of predictors on SOC concentration for different plant functional types.

3.2. Data clustering based on environmental factors

To develop the calibration groups for MIMICS-ENV, we partitioned the top three important abiotic factors, which are soil bulk density, MAT and MAP, into six distinct clusters using K-means (see Section 2.3). The resulting characteristics and spatial distribution of SOC belonging to these six clusters are illustrated in Figure 4.

Notably, a substantial majority of forests were assigned to clusters 2 and 6 (Figure 4a), while woodland, shrubland, and grassland observations were distributed across the remaining four clusters. Among these clusters, cluster 5 exhibits the lowest SOC concentration, while SOC of cluster 1 and 3 display a comparable pattern but spread across different biomes. Conversely, distribution of SOC concentration in clusters 2, 4, and 6 shows more pronounced variability (Figure 4c).

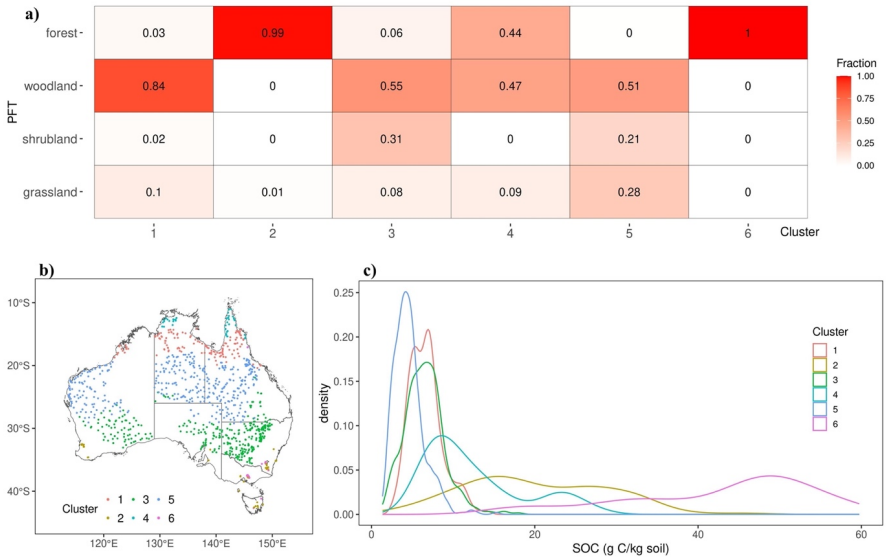

Figure 4. a) Fraction of different PFT in each cluster divided based on environmental factors; b) spatial distribution of SOC observations from different environmental clusters and c) density plot of observed SOC concentration for different clusters.

3.3. Evaluation of model performance

All models employed in this study (RF, K-means + MLR, MIMICS-PFT and MIMICS-ENV) predicted SOC concentration well for both training data and test data (Figure 5). As anticipated, sample data versus in-sample training or calibration data. When using test data, the mean value of R^2 for all models ranges from 0.82 to 0.94, mean LCCC ranges from 0.90 to 0.97, mean RMSE ranges from 2.88 to 4.51 g C/kg soil, and mean MAE ranges from 1.55 to 2.57 g C/kg soil.

The machine learning models outperformed MIMICS in predicting SOC concentration, regardless of the optimisation approach taken. Particularly, the RF model demonstrated the most accurate predictions characterized by higher R^2 and LCCC values and lower RMSE and MAE values for both training and test data. While MIMICS-ENV displayed performance similar to that of MIMICS-PFT in SOC concentration predictions based on RMSE and MAE, the former exhibited slightly superior median R^2 and LCCC values but with a higher variability (Figure 5).

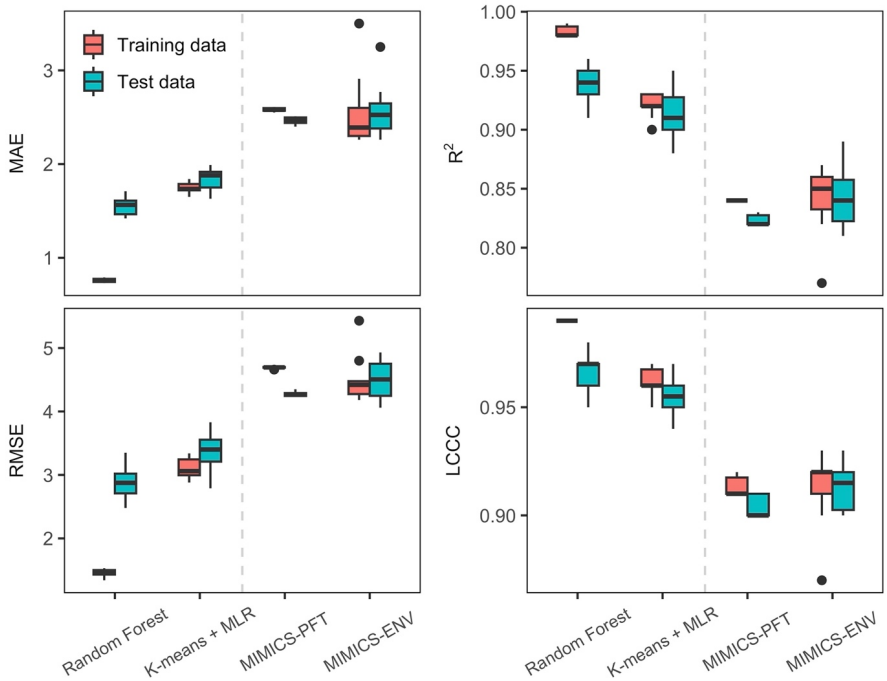

Figure 5. Performance metrics of SOC concentration predictions. Units for MAE and RMSE are g C/kg soil. Centre line represents median value, and upper and lower box boundaries represent third and first quartile of metrics from cross-validation. Whiskers extend to the smallest and largest values within 1.5 times the interquartile range.

SOC concentration in forest soil exhibited significantly higher predictability than those in non-forest (woodland, shrubland and grassland) soil, evidenced by higher R^2 (ranging from 0.58 to 0.91) and LCCC (ranging from 0.75 to 0.95) for test data (Figure 6). Machine learning models surpassed MIMICS in predicting SOC concentration for both forest and non-forest soils. Notably, MIMICS-ENV outperformed MIMICS-PFT in SOC concentration predictions, particularly in non-forest soils.

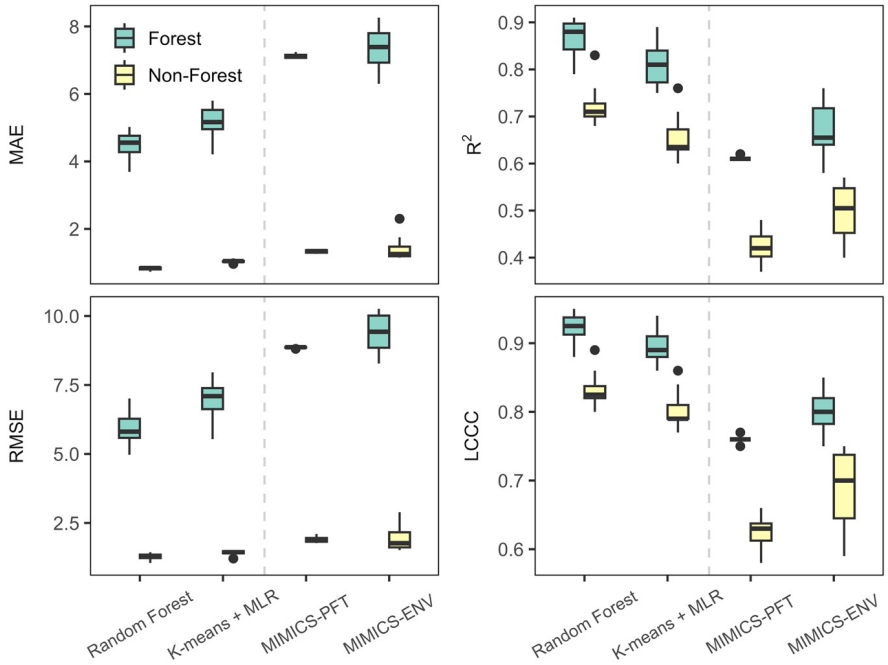

Figure 6. Performance metrics of SOC concentration predictions for forest and non-forest (woodland, shrubland and grassland) soils in test (out-of-sample) data. Unit for MAE and RMSE is g C/kg soil. Centre line represents median value, and upper and lower box boundaries represent third and first quartile of metrics from cross-validation. Whiskers extend to the smallest and largest values within 1.5 times the interquartile range.

3.4. Estimations of terrestrial SOC stocks

Using the best fitted models after cross-validation (see Section 2.6 for details), we estimated the total amount of SOC stocks in the top 30 cm for the whole Australia continent at a spatial resolution of 0.05□by 0.05□ The optimized parameters used for MIMICS-PFT and MIMICS-ENV at continental scale are shown in Table 3.

Table 3. Optimized parameter ranges of MIMICS for cross-validation. Values in brackets were used for estimating SOC stocks at continental scale. See Table 1 for further explanations of each parameter.

Model	PFT/Cluster	a_v	a_k	xdesorp	xbeta	xdiffsoc
MIMICS-PFT	Grassland	4.36-18.11 (5.45)	4.42-19.11 (5.62)	1.90-3.0 (2.97)	1.06-1.42 (1.06)	16.21-29.90 (29.3)
	Shrubland	12.15-17.91 (12.46)	14.46-18.87 (16.80)	1.54-2.92 (2.58)	1.14-1.27 (1.24)	20.21-29.96 (29.73)
	Woodland	8.41-17.01 (10.92)	9.35-16.99 (12.73)	1.12-1.23 (1.10)	1.12-1.23 (1.18)	20.17-29.96 (23.91)
	Forest	3.15-8.56 (4.70)	12.61-19.69 (13.53)	0.39-3.0 (1.36)	1.42-1.88 (1.35)	11.55-27.70 (10.20)
MIMICS-ENV	Cluster 1	5.23-13.82 (10.189)	6.08-17.80 (11.93)	1.62-2.85 (1.84)	1.07-1.20 (1.07)	0.00-29.81 (28.80)
	Cluster 2	3.56-10.76 (7.60)	7.36-18.24 (15.70)	1.01-2.94 (2.07)	1.05-1.07 (1.05)	3.61-12.75 (6.91)
	Cluster 3	8.31-10.52 (8.48)	15.98-19.91 (19.66)	1.84-2.83 (2.25)	1.36-1.52 (1.52)	10.83-29.45 (26.25)
	Cluster 4	2.47-5.52 (5.10)	6.44-16.80 (13.52)	0.54-1.78 (0.92)	1.21-1.74 (1.42)	14.75-28.91 (20.37)
	Cluster 5	12.24-20.57 (19.55)	10.90-17.56 (17.56)	2.89-3.0 (2.98)	1.05-1.06 (1.05)	25.32-29.83 (25.75)
	Cluster 6	3.25-7.18 (6.40)	7.73-18.23 (15.86)	1.91-2.97 (2.73)	1.05-1.09 (1.09)	6.19-28.57 (15.47)

Descriptive statistics of predicted terrestrial SOC stocks at 0-30 cm soil depth are shown in Table 4. Forests have the largest mean SOC stocks ranging from 70.3 to 113.9 t ha^{-1} by all models, and shrubland is estimated to have the lowest mean SOC stocks. The distributions of predicted continental SOC stocks by all models are positively skewed with most estimated SOC stocks less than 50 t ha^{-1} (Figure 7a), and SOC stocks at peak density predicted by MIMICS-ENV and MIMICS-PFT are smaller than those predicted by the two machine learning approaches.

As expected, all models consistently projected larger SOC stocks in the southeast region, southwest corner and Tasmania, and consistently indicated lower SOC stocks in central and western Australia (Figure 7b). Among the models, K-means coupled with multiple linear regression consistently provided the highest SOC estimations across all vegetation types, while MIMICS-PFT model consistently yielded the lowest mean SOC stocks.

The ensemble estimate of SOC stocks (Figure 7c) shows a similar distribution pattern as that generated by single model. SOC stocks of the ensemble range from 10.0 to 180.4 t ha^{-1} with an average value of 30.3 t ha^{-1}. Coefficient of variation calculated as the ratio of standard deviation to mean across the four estimates (Figure 7d) is positively correlated with the ensemble mean estimate. That is, soils with higher SOC stocks exhibit greater variability in SOC predictions among different models. Note also that the variability of estimates tends to be smaller in areas with denser numbers of observations (Figure 7d).

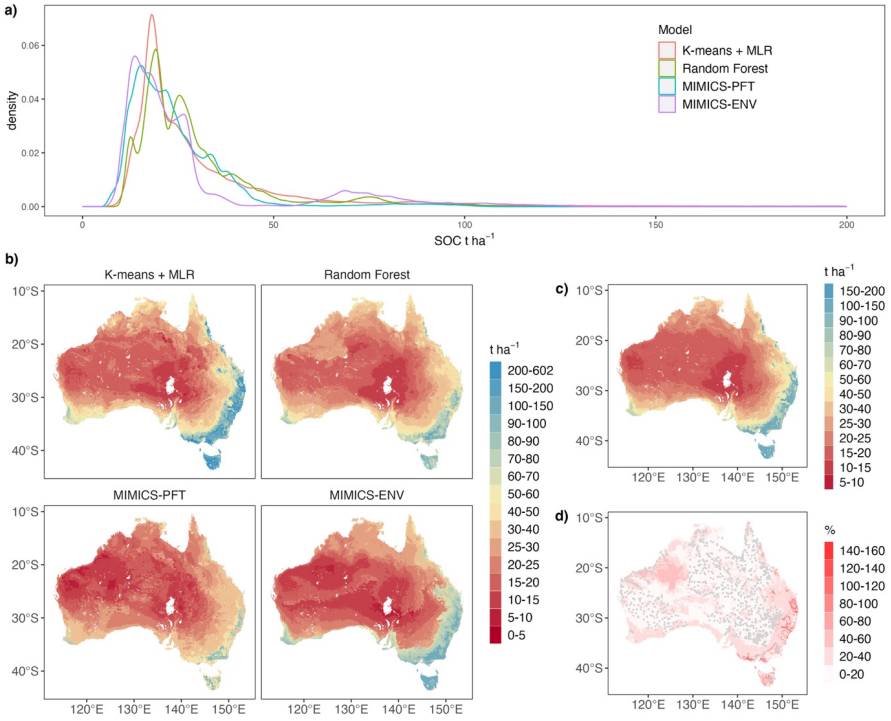

Deleted:

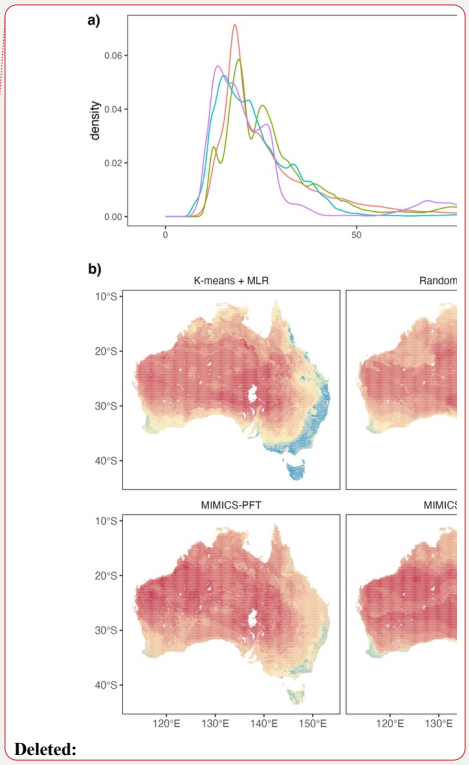

Figure 7. Estimated Australian terrestrial SOC stocks (t ha^{-1}) for top 30 cm soil and ensemble statistical characteristics: a) density plot of estimated terrestrial SOC stocks by all models, noting that only stocks less than 200 t ha^{-1} are shown for better comparison of the distribution; b) estimated SOC stocks by each model; c) estimated SOC stocks of the ensemble; d) coefficient of variation of the ensemble estimates of SOC stocks. Grey points represent locations of SOC observations.

Table 4. Descriptive statistics of estimated terrestrial SOC stocks (t ha^{-1}) at 0-30 cm soil. Min. and Max. are minimum and maximum value, respectively. 1st Qu and 3rd Qu are first and third quartile, respectively.

	PFT	Min.	1st Qu	median	mean	3rd Qu	Max.
K-means + MLR	grassland	4.2	17.9	21.2	41.5	42.5	601.1
	shrubland	7.2	16.4	19.3	23.6	24.4	472.2
	woodland	7.1	20.1	26.1	33.3	33.7	483.1
	forest	18.0	51.3	95.2	113.9	153.4	474.0
	all	4.2	18.1	23.6	38.2	36.7	601.1
Random Forest	grassland	10.4	18.5	26.0	30.4	37.2	125.3
	shrubland	10.3	17.0	19.6	21.4	24.4	104.4
	woodland	10.5	20.3	25.8	28.2	32.4	122.1
	forest	29.3	55.0	82.3	78.4	97.0	161.7
	all	10.3	18.9	25.0	29.8	33.7	161.7
	grassland	10.8	16.4	24.1	25.1	33.3	58.7

MIMICS-PFT	shrubland	6.5	12.2	15.5	16.5	20.6	56.5
	woodland	7.8	17.4	21.2	22.1	25.9	61.4
	forest	17.9	44.5	77.4	70.3	88.5	109.9
	all	6.5	15.7	21.2	24.3	28.9	109.9
MIMICS-ENV	grassland	6.8	13.7	18.7	29.9	27.6	124.0
	shrubland	6.7	13.4	16.7	18.3	20.2	131.9
	woodland	8.1	18.0	24.0	27.5	28.0	131.6
	forest	15.8	35.7	90.4	79.4	106.5	134.1
	all	6.7	15.0	20.2	28.9	27.5	134.1
Ensemble	grassland	11.4	17.1	21.1	31.7	36.3	180.4
	shrubland	10.0	15.2	17.3	20.0	21.7	170.4
	woodland	11.0	18.8	24.4	27.8	30.0	168.0
	forest	22.0	46.8	93.1	85.5	112.7	166.3
	all	10.0	17.2	22.2	30.3	31.5	180.4

4. Discussion

4.1. Relative importance of predictors on SOC variations

Extensive research has been conducted to discern the factors that govern SOC concentration/stocks. Among the commonly employed predictors for SOC spatial variations, climate, organisms, topography, parent material, and soil properties are prominent (Wiesmeier et al., 2019). Within this study, we conducted a comparative assessment of the significance of key variables, namely MAT, MAP, NPP, soil clay content and bulk density, in driving variations in SOC in Australia. Although the number of predictors utilized in our approach is fewer than that employed in most digital mapping methodologies, our models show good performance in predicting SOC in Australia (Figure 5 and 6) and its strength lies in the potential for a more direct comparison between empirical and process-based models.

Consistent with the result by Hobley et al., (2015) on the soils from eastern Australia, this study identified soil bulk density as an important predictor of SOC concentration at continental scale (Figure 3). However, the relationship is largely interactive between soil bulk density and soil carbon concentration (Murphy, 2015). Higher concentrations of soil organic matter facilitate soil aggregation formation and increase soil porosity, which results in lower bulk density. Meanwhile, a soil with reduced bulk density exhibits higher permeability for water and oxygen, which enhances plant root growth and SOC dynamics. Physically, the bulk density of organic matter is less than 1 g cm^{-3}, much lower than soil mineral solids with a density of 2.66 g cm^{-3}, therefore lower bulk density soils usually have higher SOC concentration (Marshall and Holmes, 1988).

Across the Australia continent, MAT emerges as the second most influential factor governing SOC variations, followed by NPP, MAP, and clay content. This sequence of significance diverges from the findings of Walden et al. (2023), where the order of importance was observed as NPP > clay content > MAP > MAT on a continental scale in Australia. The number of predictors used in their study is much higher than that in our study, which may affect the contribution of given predictors in SOC variation (Guo et al., 2019). This discrepancy might

however be attributable to the utilization of observations encompassing both terrestrial and blue carbon ecosystems in their study. Clay emerges as key driver mainly in the groups where aquatic plants (e.g., seagrass, tidal marsh) appeared. The more extensive dataset encompassing the eastern coastline, characterized by greater variability and abundance of NPP input, potentially elevates NPP to a dominant role in influencing SOC variations within their study.

For SOC in different vegetation types (Figure 3), soil bulk density and MAT are more important than other factors in forest, and all factors except clay content showed similar importance in predicting SOC concentration in grassland. NPP and MAP dominate the SOC variations in woodland and shrubland. Climate conditions as represented by MAT and MAP exert their impact on SOC in all vegetation types. It was proposed that the primary climatic determinant of SOC variation hinges on the primary constraint affecting SOC production and turnover (Hobley et al., 2016). In this study, most shrublands and woodlands are distributed in arid and semi-arid regions characterized by limited precipitation, which leads to water stress in surface soil, limiting plant productivity and reducing soil C input (Hobley et al., 2015). Consequently, MAP and NPP exhibited relatively higher influence on SOC variations in soils under these vegetation types. In contrast, forest SOC observations are mainly distributed in areas with relatively lower temperatures, therefore experience constrained microbial metabolism, leading to reduced decomposition rates and the high accumulation of SOC (Wynn et al., 2006). Consequently, MAT emerges as a key factor influencing SOC variations in forests. Furthermore, it is noteworthy that soil bulk density plays a crucial role in determining SOC distribution within forest, where it is found to be significantly lower compared to other vegetation types. This lower soil bulk density likely improves oxygen availability to soil microbial communities, and facilitates the formation of microaggregates to enhance the preservation of SOC within the soil matrix (Bronick and Lal, 2005). Consequently, it effectively contributes to elevated SOC concentration levels in forested areas.

PFT is the only categorical predictor for SOC concentration in this study. SOC is mainly derived from plant C input through above-/belowground tissues, and SOC turnover and storage are influenced by plant traits like plant growth rate and chemical and physical composition (De Deyn et al., 2008; Faucon et al., 2017). With shared representation of similar plant traits, PFT is widely used in process-based models (Poulter et al., 2015; Famiglietti et al., 2023). It was found that the vertical distribution of SOC is highly related to PFT due to the different root distribution and above- and belowground allocation (Jobbágy and Jackson, 2000). However, our study is limited by the absence of SOC observations at multiple soil depths, restricting the analysis to the spatial distribution of SOC at 30 cm soil depth. The influence of PFT on SOC concentration at this particular depth appears relatively insignificant (Figure 3), casting doubt on the effectiveness of optimizing parameters of process-based models for individual PFT (Cranko Page et al., 2023). Considering this, employing the top 3 influential abiotic predictors, soil bulk density, MAT, and MAP, we partitioned all observations into six distinct clusters using K-means. It was anticipated that SOC ranges within each cluster would be narrow due to the high similarity of these three predictors within each group. However, the distribution of SOC

in clusters 2, 4, and 6 exhibited considerable variability (Figure 4). Given that these clusters are predominantly composed of forests, it becomes apparent that these three abiotic factors alone are insufficient to fully characterize the intricacies of forest SOC concentration. It was found that elevation and evapotranspiration also drive the variation of forest SOC in Australia (Walden et al., 2023), and taking them into account might potentially increase the predictability of forest SOC.

4.2. Model evaluation and comparison with other studies

Although the predictors used for machine learning models are not exactly same as the inputs of MIMICS, the missing factors (e.g., MAP) were used for parameter optimization of MIMICS-ENV, making the predictions dependent on similar information and so comparable to some extent. Besides, our study presented clear evaluation metrics for out-of-sample validation, enabling a more robust assessment of model performance when applied to new datasets.

Based on the performance metrics of test data, the machine learning models performed remarkably well (Figure 5). The R^2 suggested that both machine learning models can explain more than 90% of SOC variability across sites, and random forest did the best job with greatest R^2 and LCCC, and lowest MAE and RMSE. Random forest algorithms were widely adopted in predicting spatial-temporal SOC dynamics and produced moderately good performance regionally and globally. For example, Wang et al. (2022) applied random forest to estimate SOC stocks in south-eastern Australia and explained 69% of the variation of current SOC stocks. Nyaupane et al. (2023) trained a random forest model using global SOC observations and explained 61% of SOC variation. The good performance of random forest might be attributed to reduced susceptibility to over-fitting and better capacity to manage the hierarchical non-linear relationships that exist between SOC and environmental predictors (Wang et al., 2018b). Other machine learning methods have been applied to predict continental SOC stocks in Australia. For example, Walden et al. (2023) trained regression-tree algorithm CUBIST to predict SOC stocks for top 30 cm soil using the harmonised datasets. The mean LCCC and RMSE for out-of-sample validation in their study was 0.78 and 0.20 respectively when $\log_{10}$ transformed SOC (t ha^{-1}) values were used. Wadoux et al. (2023) applied quantile regression forest to predict SOC stocks at multiple soil depths. The prediction accuracy decreased dramatically for deeper depth intervals with the greatest R^2 (0.53) at 0-5 cm soil. The better results in this study may be attributed to the removal of cropland ecosystems, which are clearly highly managed and so less predictable. Agricultural practices greatly affect SOC stocks in Australia and add the complexity to the relationship between SOC and environmental factors (Luo et al., 2010). Models using environmental predictors without representation of land use management are unlikely to be able to fully capture the SOC dynamics in croplands (Abramoff et al., 2022).

Although MIMICS was not as accurate as machine learning models in simulating spatial variation of SOC concentration in Australia, it did well at continental scale with mean R^2 at 0.82 and 0.84 for MIMICS-PFT and MIMICS-ENV, respectively (Figure 5), much greater than

607 the values (<0.4) obtained by Abramoff et al. (2022) who applied a different microbial explicit
608 model to Australian SOC dataset. Georgiou et al. (2021) found that there was a mismatch
609 between observations and MIMICS in the role of different environmental controls on SOC
610 variability at global scale. In their study, NPP and MAT had the most explanatory power for
611 SOC stocks from MIMICS, while clay content had the most explanatory power for global SOC
612 observations, which limits the predictability of SOC using MIMICS in their study. However, in
613 our study, NPP and MAT rather than clay content played a greater role in observed SOC
614 variations, perhaps contributing to a better performance of MIMICS in Australia. It also means
615 that SOC estimates in our study are highly sensitive to the estimates of NPP. In this study, we
616 used MODIS NPP product (Running and Zhao, 2021) and did not account for the loss of NPP
617 due to human activities, which may likely influence the optimized estimates of some model
618 parameters, and the uncertainties of simulated SOC concentration. Future studies would ideally
619 use multiple NPP products to quantify the impacts of NPP uncertainties in simulating SOC
620 variation in Australia.
621
622 The modest performance of process-based model MIMICS relative to machine learning models
623 could potentially be attributed to the absence of explicit representation of MAP. The
624 augmentation of MAP within parameter optimization in MIMICS-ENV did allow improved
625 performance compared to MIMICS-PFT, particularly within non-forest regions where the
626 importance of MAP rivals or surpasses that of temperature. Precipitation is a determinant of
627 plant productivity, especially in arid and semi-arid regions. Besides, arid regions with limited
628 precipitation are characterized by lower weathering rate limiting the formation of mineral-
629 associated soil carbon (Doetterl et al., 2015). Hence, we assume that introducing the effect of
630 moisture to MIMICS could contribute to more accurate prediction of SOC, as compared with
631 just taking MAP into account for parametrization, especially in arid and semiarid regions.
632
633 All models produced lower MAE and RMSE for non-forest SOC but higher R^2 and LCCC for
634 forest SOC (Figure 6). SOC in forest is more abundant and variable compared to SOC in other
635 vegetation types even when climate conditions are similar, which leads to greater absolute error
636 in the estimated forest SOC than in other vegetation types. However, in terms of the consistency
637 and concordance between the pattern of observations and predictions, all models show higher
638 ability to predict SOC in forest. Forests, given that they are less perturbed ecosystems, might
639 show greater SOC predictability due to the reduced influence of direct anthropogenic
640 disturbances. Grasslands, shrublands, and woodlands, predominantly situated in Australian
641 rangelands may experience extensive grazing and land management. Primarily, grazing reduces
642 soil carbon input by consumption of aboveground biomass and accelerate SOC decomposition
643 through input of nutrient-enriched animal waste. This introduces additional uncertainties to our
644 modelled SOC estimates, since C input is represented solely by NPP without accounting for the
645 impact of grazing and land managements. Moreover, the cascading effects of grazing extend to
646 potential alterations in plant composition and structural attributes, inducing consequential shifts
647 in litter properties that modulate soil carbon decomposition kinetics (Lunt et al., 2007; Bai and
648 Cotrufo, 2022). The disturbances triggered by grazing manifest in soil carbon pools, leading to

a state of disequilibrium rather than adhering to the assumption of SOC convergence toward equilibrium, as embraced in this study's framework. Notably, forests, as relatively undisturbed natural ecosystems, demonstrate a better coherence with the equilibrium assumption, rendering their SOC more amenable to prediction through environmental drivers.

4.3. Spatial prediction of SOC stocks in Australia

We produced gridded SOC stocks across Australia using the models validated in this study and an ensemble estimate as the average of four models (Figure 7). Among the models, K-means coupled with multiple linear regression produced the largest mean SOC stocks both at continental scale and for all vegetation types. In contrast, RF and MIMICS with different parameterization approaches produced lower SOC stock estimations (Table 4). The mean terrestrial SOC stocks estimated by random forest and MIMICS are comparable with that estimated by Australian baseline map, which was generated using machine learning algorithm, reporting mean SOC stocks at 29.7 t ha^{-1} with 95% confidence limits of 22.6 and 37.9 t ha^{-1} (Viscarra Rossel et al., 2014). However, SOC stocks might be underestimated by these methods because of the scarcity of data from the most productive temperate forest both in the baseline map (Bennett et al., 2020) and in our study. Parameter optimization process of MIMICS and the training process of random forest are greatly affected by data used to train the model. Most SOC observations in this study were sourced from arid and semiarid regions, characterized by relatively low SOC content. As a result, the models' ability to predict SOC stocks beyond the observed data range is somewhat constrained. PFT was found to be less important than other environmental factors in driving spatial SOC variations (Figure 3), so it was perhaps not surprising that applying parameters optimized for each plant functional type to the regions with same PFT but broader climate conditions led to inferior results than applying parameters optimized for each environmental group.

The utilization of linear regression in K-means + MLR generated SOC estimates beyond the range of observations, particularly in eastern Australia where environmental conditions deviate from the training data. The mean SOC stocks estimated by K-means + MLR (38.2 t ha^{-1}) are higher than those of the other models employed in this study, and align closely with the mean value 36.2 t ha^{-1} reported by Walden et al. (2023) who updated the Australian baseline SOC map (Viscarra Rossel et al., 2014) by incorporating additional SOC observations from forests and coastal marine ecosystems. However, caution is required when interpreting extreme values derived from the K-means + MLR, such as the instance of grassland SOC stocks reaching 601 t ha^{-1} (Table 4). These values raise concerns about the reliability of this approach when extrapolating out-of-sample. Though there is a positive relationship between NPP and SOC observations in this study, SOC accumulation cannot continuously increase linearly in the regions where environmental conditions seem highly conducive to SOC formation. The greater amount of carbon input in eastern Australia might trigger the acceleration of microbial decomposition because of a priming effect, and lead to a decreased accumulation of SOC stocks (Ren et al., 2022). The existence of SOC saturation also implies that SOC cannot be

accumulated without limit (Georgiou et al., 2022; Viscarra Rossel et al., 2023). In light of these complexities, applying linear regression to predict SOC stocks, especially under the extreme environmental conditions, should be undertaken with care.

Continentally, higher SOC stocks were estimated for the southwest corner and southeast Australia (Figure 7), aligning with other SOC maps for Australia (Wadoux et al., 2023; Walden et al., 2023). These regions are characterized by lower temperature and higher precipitation, therefore high SOC accumulation appeared because of high carbon input of NPP and low decomposition rate. However, the high variability of SOC estimates among the four models in these regions should be highlighted (Figure 7d), along with the difference of magnitudes between the estimates in this study and other Australian SOC products (Viscarra Rossel et al., 2014; Walden et al., 2023). Despite inherent differences in model structures, the scarcity of observations in these regions likely contributes to the large uncertainties in SOC estimates. Forest has the largest mean SOC stocks ranging from 70.3 to 113.9 t ha^{-1} estimated by four models in this study. Around 75% of the forest SOC is from soil under Eucalypt open forest, and mean SOC stocks under this type of forest were estimated to be 87.5 t ha^{-1} (63.8 -119.6 t ha^{-1} for 95% confidence interval) (Walden et al., 2023). Shrublands are estimated to have the lowest mean SOC stocks, and more than 90% of shrub SOC observations are from soil under Acacia shrubland and Chenopod shrubland, which rank at the bottom of SOC stocks among different vegetation types (Walden et al., 2023). The low SOC in shrubland is probably due to low carbon input because of limited rainfall (MAP < 280 mm). Though the mean SOC stocks in non-forest regions are much smaller than that for forest, the greater area of vegetation cover results in considerable total SOC stocks, highlighting the importance of carbon building and maintaining via improved managements in these areas. Greater variability of SOC estimates among different models appears in the regions where SOC stocks are higher (Figure 7). The sparsity of SOC observations is a primary contributor to the uncertainties associated with SOC estimates in these regions, highlighting the importance on continual collection of data to better constrain models' behaviour. This imperative is especially pronounced in regions covered by forests, as forested soils exhibit substantial SOC stocks, amplifying the significance of abundant and accurate data acquisition in these specific ecosystems.

5. Conclusion

We compared the performance of two machine learning models, and one process-based microbial model employing two parameterization approaches, to explain the spatial variation of SOC concentration in the top 30 cm soil in Australia. We found that climate conditions and NPP contribute more than soil clay content in predicting SOC concentration in Australia.

Validation results affirm that with appropriate filtering of data (e.g. removing highly managed crop ecosystems) models can predict SOC concentration at a continental scale with reasonably high reliability, achieving explained variances exceeding 80% for out-of-sample test data, with random forest showing highest prediction accuracy. Notably, all models show higher R^2 in

prediction of SOC in forest than in non-forest soils. MIMICS, with parameters optimized for different environmental clusters, performed better in SOC prediction than MIMICS with parameters optimized for different PFT, especially in non-forest regions.

All models broadly agree on the spatial distribution of SOC stocks, with higher SOC stocks concentrated in the southeast and southwest regions of Australia. However, the variations in estimated values need to be acknowledged, particularly in highly productive regions. Among these estimates, K-means algorithm coupled with multiple linear regression yields the highest mean SOC stocks estimate, while the MIMICS-PFT model generates the lowest estimate. Considerable disagreement of the maximum and minimum SOC stock values predicted by all models exists partly because models are less constrained by observations in these environments, highlighting the need for continued observational campaigns.

Our investigation has revealed significant disparities in estimated SOC stocks when different methodologies were employed. This highlights the need for a critical re-evaluation of land management strategies that heavily depend on SOC estimates derived from a single approach. The incorporation of an ensemble of SOC estimates is more likely to effectively capture elements of the uncertainty associated with SOC estimations, providing a more robust basis for informing strategies in soil carbon management and climate change mitigation.

Code availability

Source Code of vertically resolved MIMICS can be accessed at https://github.com/Wanglingfei170/MIMICS.git. Codes for data analysis and machine learning can be accessed by contacting the correspondence author.

Data availability

The SOC observations described in Viscarra Rossel et al. (2014) are not publicly available but are available from Raphael A. Viscarra Rossel (r.viscarra-rossel@curtin.edu.au) on reasonable request. All other data used in this study are publicly accessible and the specific references are provided in Section 2.4.

Author contribution

Conceptualization: LW, GA, Y-PW, AP; Methodology: LW, GA, Y-PW; Investigation: LW, RAVR; Formal analysis and Visualization: LW; Writing-original draft preparation: LW; Writing-review & editing: LW, GA, Y-PW, AP, RAVR.

Competing interests

The co-author Raphael A. Viscarra Rossel is a member of the editorial board of SOIL.

Deleted: the CSIRO data portal https://doi.org/10.25919/843a-w584 (Wang et al., 2021).

Deleted: of these databases

Acknowledgements

LW thanks the China Scholarship Council and the University of New South Wales for financial support during her PhD study. RAVR and Y-PW thank the Australian Research Council's Discovery Projects scheme (project DP210100420) for funding. LW, GA and AP thank the ARC Centre of Excellence for Climate Extremes for supporting this work (CE170100023).

Reference

Abramoff, R. Z., Guenet, B., Zhang, H., Georgiou, K., Xu, X., Viscarra Rossel, R. A., Yuan, W. and Ciais, P.: Improved global-scale predictions of soil carbon stocks with Millennial Version 2. Soil Biol Biochem, 164, 108466, https://doi.org/10.1016/j.soilbio.2021.108466, 2022.

Abs, E. and Ferrière, R.: Modeling microbial dynamics and heterotrophic soil respiration: Effect of climate change. Biogeochemical cycles: ecological drivers and environmental impact, 103-129, https://doi.org/10.1002/9781119413332.ch5, 2020.

Adhikari, K., Mishra, U., Owens, P., Libohova, Z., Wills, S., Riley, W., Hoffman, F. and Smith, D.: Importance and strength of environmental controllers of soil organic carbon changes with scale. Geoderma, 375, 114472, https://doi.org/10.1016/j.geoderma.2020.114472, 2020.

Bai, Y. and Cotrufo, M. F.: Grassland soil carbon sequestration: Current understanding, challenges, and solutions. Science, 377, 603-608, doi: 10.1126/science.abo2380, 2022.

Bennett, L. T., Hinko-Najera, N., Aponte, C., Nitschke, C. R., Fairman, T. A., Fedrigo, M. and Kasel, S.: Refining benchmarks for soil organic carbon in Australia's temperate forests. Geoderma, 368, 114246, https://doi.org/10.1016/j.geoderma.2020.114246, 2020.

Bissett, A., Fitzgerald, A., Meintjes, T., Mele, P. M., et al.: Introducing BASE: the biomes of Australian soil environments soil microbial diversity database. GigaScicence, 5, s13742–016–0126–5. https://doi.org/10.1186/s13742-016-0126-5, 2016.

Bossio, D., Cook-Patton, S., Ellis, P., Fargione, J., Sanderman, J., Smith, P., Wood, S., Zomer, R., Von Unger, M. and Emmer, I.: The role of soil carbon in natural climate solutions. Nat Sustain, 3, 391-398, https://doi.org/10.1038/s41893-020-0491-z, 2020.

Breiman, L.: Random forests. Machine learning, 45, 5-32, https://doi.org/10.1023/A:1010933404324, 2001.

Bronick, C. J. and Lal, R: Soil structure and management: a review. Geoderma, 124, 3-22, https://doi.org/10.1016/j.geoderma.2004.03.005, 2005.

Cranko Page, J., Abramowitz, G., De Kauwe, M. G. and Pitman, A. J.: Are plant functional types fit for purpose? Geophys Res Lett, 51, e2023GL104962, https://doi.org/10.1029/2023GL104962, 2024.

Chandel, A. K., Jiang, L. and Luo, Y.: Microbial Models for Simulating Soil Carbon Dynamics: A Review. J Geophys Res-Biogeo, e2023JG007436, https://doi.org/10.1029/2023JG007436, 2023.

De Deyn, G. B., Cornelissen, J. H. and Bardgett, R. D.: Plant functional traits and soil carbon sequestration in contrasting biomes. Ecol Lett, 11, 516-531, https://doi.org/10.1111/j.1461-0248.2008.01164.x, 2008.

Debeer, D. and Strobl, C.: Conditional permutation importance revisited. BMC bioinformatics, 21, 1-30, https://doi.org/10.1186/s12859-020-03622-2, 2020.

Doetterl, S., Stevens, A., Six, J., Merckx, R., Van Oost, K., Casanova Pinto, M., Casanova-Katny, A., Muñoz, C., Boudin, M. and Zagal Venegas, E.: Soil carbon storage controlled by interactions between geochemistry and climate. Nat Geosci, 8, 780-783, https://doi.org/10.1038/ngeo2516, 2015.

Duan, Q., Gupta, V. K. and Sorooshian, S.: Shuffled complex evolution approach for effective and efficient global minimization. J Optim Theory Appl, 76: 501-521, https://doi.org/10.1007/BF00939380, 1993.

Famiglietti, C. A., Worden, M., Quetin, G. R., Smallman, T. L., Dayal, U., Bloom, A. A., Williams, M. and Konings, A. G.: Global net biome CO_2 exchange predicted comparably well using parameter–environment relationships and plant functional types. Glob Change Biol, 29, 2256-2273, https://doi.org/10.1111/gcb.16574, 2023.

Faucon, M.-P., Houben, D. and Lambers, H.: Plant functional traits: soil and ecosystem services. Trends Plant Sci, 22, 385-394, https://doi.org/10.1016/j.tplants.2017.01.005, 2017.

Georgiou, K., Malhotra, A., Wieder, W. R., Ennis, J. H., Hartman, M. D., Sulman, B. N., Berhe, A. A., Grandy, A. S., Kyker-Snowman, E. and Lajtha, K.: Divergent controls of soil organic carbon between observations and process-based models. Biogeochemistry, 156, 5-17, https://doi.org/10.1007/s10533-021-00819-2, 2021.

Georgiou, K., Jackson, R. B., Vindušková, O., Abramoff, R. Z., Ahlström, A., Feng, W., Harden, J. W., Pellegrini, A. F., Polley, H. W. and Soong, J. L.: Global stocks and capacity of mineral-associated soil organic carbon. Nat Commun, 13, 3797, https://doi.org/10.1038/s41467-022-31540-9, 2022.

Grace, P. R., Post, W. M. and Hennessy, K.: The potential impact of climate change on Australia's soil organic carbon resources. Carbon Balance Manag, 1, 1-10, https://doi.org/10.1186/1750-0680-1-14, 2006.

Grundy, M., Viscarra Rossel, R. A., Searle, R., Wilson, P., Chen, C. and Gregory, L.: Soil and landscape grid of Australia. Soil Res, 53, 835-844, https://doi.org/10.1071/SR15191, 2015.

Guo, Z., Adhikari, K., Chellasamy, M., Greve, M. B., Owens, P. R. and Greve, M. H.: Selection of terrain attributes and its scale dependency on soil organic carbon prediction. Geoderma, 340, 303-312, https://doi.org/10.1016/j.geoderma.2019.01.023, 2019.

Heung, B., Ho, H. C., Zhang, J., Knudby, A., Bulmer, C. E. and Schmidt, M. G.: An overview and comparison of machine-learning techniques for classification purposes in digital soil mapping. Geoderma, 265, 62-77, https://doi.org/10.1016/j.geoderma.2015.11.014, 2016.

Hobley, E., Wilson, B., Wilkie, A., Gray, J. and Koen, T.: Drivers of soil organic carbon storage and vertical distribution in Eastern Australia. Plant Soil, 390, 111-127, https://doi.org/10.1007/s11104-015-2380-1, 2015.

Hobley, E. U., Baldock, J. and Wilson, B.: Environmental and human influences on organic carbon fractions down the soil profile. Agric Ecosyst Environ, 223, 152-166, https://doi.org/10.1016/j.agee.2016.03.004, 2016.

Jackson, R. B., Lajtha, K., Crow, S. E., Hugelius, G., Kramer, M. G. and Piñeiro, G.: The ecology of soil carbon: pools, vulnerabilities, and biotic and abiotic controls. Annual review of ecology, evolution, and systematics, 48, 419-445, https://doi.org/10.1146/annurev-ecolsys-112414-054234, 2017.

Jeffrey, S. J., Carter, J. O., Moodie, K. B. and Beswick, A. R.: Using spatial interpolation to construct a comprehensive archive of Australian climate data. Environ Model Softw, 16, 309-330, https://doi.org/10.1016/S1364-8152(01)00008-1, 2001.

Jenny, H.: Factors of soil formation: a system of quantitative pedology, Agron. J., 33, 857-858, https://doi.org/10.2134/agronj1941.00021962003300090016x, 1941.

Jobbágy, E. G. and Jackson, R. B.: The Vertical Distribution of Soil Organic Carbon and Its Relation to Climate and Vegetation. Ecol Appl, 10, 423-436, https://doi.org/10.1890/1051-0761(2000)010[0423:TVDOSO]2.0.CO;2, 2000.

Keskin, H., Grunwald, S. and Harris, W. G.: Digital mapping of soil carbon fractions with machine learning. Geoderma, 339, 40-58, https://doi.org/10.1016/j.geoderma.2018.12.037, 2019.

Lamichhane, S., Kumar, L. and Wilson, B.: Digital soil mapping algorithms and covariates for soil organic carbon mapping and their implications: A review. Geoderma, 352, 395-413, https://doi.org/10.1016/j.geoderma.2019.05.031, 2019.

Lawrence, I. and Lin, K.: A concordance correlation coefficient to evaluate reproducibility. Biometrics, 45, 255-268, https://doi.org/10.2307/2532051, 1989.

Le Noë, J., Manzoni, S., Abramoff, R., Bolscher T., Bruni, E., Cardinael, R., Ciais, P., Chenu, C., Clivot, H., Derrien, D., Ferchaud, F., Garnier, P., Goll, D., Lashermes, G., Martin, M., Rasse, D., Rees, F., Sainte-Marie J., Salmon, E., Schiedung, M., Schimel, J., Wieder, W., Abiven, S., Barre, P., Cecillon, L. and Guenet, B.: Soil organic carbon models need independent time-series validation for reliable prediction. Commun Earth Environ, 4, 158, https://doi.org/10.1038/s43247-023-00830-5, 2023.

Lee, J., Viscarra Rossel, R. A., Zhang, M., Luo, Z. and Wang, Y. P.: Assessing the response of soil carbon in Australia to changing inputs and climate using a consistent modelling framework. Biogeosciences, 18, 5185-5202, https://doi.org/10.5194/bg-18-5185-2021, 2021.

Lefèvre, C., Rekik, F., Alcantara, V. and Wiese, L.: Soil organic carbon: the hidden potential, Food and Agriculture Organization of the United Nations (FAO), http://www.fao.org/3/a-i6937e.pdf, 2017.

Lehmann, J. and Kleber, M.: The contentious nature of soil organic matter. Nature, 528, 60-68, https://doi.org/10.1038/nature16069, 2015.

Liang, Z., Chen, S., Yang, Y., Zhou, Y. and Shi, Z.: High-resolution three-dimensional mapping of soil organic carbon in China: Effects of SoilGrids products on national modeling. Sci Total Environ, 685, 480-489, https://doi.org/10.1016/j.scitotenv.2019.05.332, 2019.

894 Lorenz, K., Lal, R. and Ehlers, K.: Soil organic carbon stock as an indicator for monitoring land
895 and soil degradation in relation to United Nations' Sustainable Development Goals. Land
896 Degrad Dev, 30, 824-838, https://doi.org/10.1002/ldr.3270, 2019.
897 Lunt, I. D., Eldridge, D. J., Morgan, J. W. and Witt, G. B.: A framework to predict the effects
898 of livestock grazing and grazing exclusion on conservation values in natural ecosystems in
899 Australia. Australian Journal of Botany, 55, 401-415, https://doi.org/10.1071/BT06178,
900 2007.
901 Luo, Y., Ahlström, A., Allison, S. D., Batjes, N. H., Brovkin, V., Carvalhais, N., Chappell, A.,
902 Ciais, P., Davidson, E. A. and Finzi, A.: Toward more realistic projections of soil carbon
903 dynamics by Earth system models. Global Biogeochem Cycles ,30, 40-56,
904 https://doi.org/10.1002/2015GB005239, 2016.
905 Luo, Z., Wang, E. and Sun, O. J.: Soil carbon change and its responses to agricultural practices
906 in Australian agro-ecosystems: a review and synthesis. Geoderma, 155, 211-223,
907 https://doi.org/10.1016/j.geoderma.2009.12.012. 2010.
908 Marshall, T. J. and Holmes, J. W.: Soil physics, 2nd ed., Cambridge University Press, New York,
909 1988.
910 McBratney, A. B., Santos, M. M. and Minasny, B.: On digital soil mapping. Geoderma, 117, 3-
911 52, https://doi.org/10.1016/S0016-7061(03)00223-4, 2003.
912 Minasny, B., McBratney, A. B., Malone, B. P. and Wheeler, I.: Digital mapping of soil carbon.
913 Advances in agronomy, 118, 1-47, https://doi.org/10.1016/B978-0-12-405942-9.00001-3,
914 2013.
915 Mishra, U. and Riley, W.: Scaling impacts on environmental controls and spatial heterogeneity
916 of soil organic carbon stocks. Biogeosciences, 12, 3993-4004, https://doi.org/10.5194/bg-12-
917 3993-2015, 2015.
918 Mokany, K., Raison, R. J. and Prokushkin, A. S.: Critical analysis of root: shoot ratios in
919 terrestrial biomes. Glob Change biol, 12, 84-96, https://doi.org/10.1111/j.1365-
920 2486.2005.001043.x, 2006.
921 Murphy, B. W.: Impact of soil organic matter on soil properties – a review with emphasis on
922 Australian soils. Soil Research, 53, 605-635, https://doi.org/10.1071/SR14246, 2015.
923 Nyaupane, K., Mishra, U., Tao, F., Yeo, K., Riley, W. J., Hoffman, F. M. and Gautam, S.:
924 Observational benchmarks inform representation of soil organic carbon dynamics in land
925 surface models. Biogeosci Discuss, 2023, 1-28, https://doi.org/10.5194/bg-2023-50, 2023.
926 Panchal, P., Preece, C., Penuelas, J. and Giri, J.: Soil carbon sequestration by root exudates.
927 Trends Plant Sci, 27, 749-757, https://doi.org/10.1016/j.tplants.2022.04.009, 2022.
928 Poulter, B., MacBean, N., Hartley, A., Khlystova, I., Arino, O., Betts, R., Bontemps, S.,
929 Boettcher, M., Brockmann, C. and Defourny, P.: Plant functional type classification for earth
930 system models: results from the European Space Agency's Land Cover Climate Change
931 Initiative. Geosci Model Dev, 8, 2315-2328, https://doi.org/10.5194/gmd-8-2315-2015,
932 2015.
933 Ren, C., Mo, F., Zhou, Z., Bastida, F., Delgado-Baquerizo, M., Wang, J., Zhang, X., Luo, Y.,
934 Griffis, T. J. and Han, X.: The global biogeography of soil priming effect intensity. Global
935 Ecol Biogeogr, 31, 1679-1687, https://doi.org/10.1111/geb.13524, 2022.

Rossel, R. V., Chen, C., Grundy, M., Searle, R., Clifford, D. and Campbell, P. The Australian three-dimensional soil grid: Australia's contribution to the GlobalSoilMap project. Soil Res, 53, 845-864, https://doi.org/10.1071/SR14366, 2015.

Rumpel, C., Amiraslani, F., Koutika, L.-S., Smith, P., Whitehead, D. and Wollenberg, E.: Put more carbon in soils to meet Paris climate pledges, Nature, 564, 32-34, https://doi.org/10.1038/d41586-018-07587-4, 2018.

Six, J., Conant, R. T., Paul, E. A. and Paustian, K.: Stabilization mechanisms of soil organic matter: Implications for C-saturation of soils. Plant Soil, 241, 155-176, https://doi.org/10.1023/A:1016125726789, 2002.

Smith, P.: Soil carbon sequestration and biochar as negative emission technologies. Glob Change Biol, 22, 1315-1324, https://doi.org/10.1111/gcb.13178, 2016.

Stockmann, U., Padarian, J., McBratney, A., Minasny, B., de Brogniez, D., Montanarella, L., Hong, S. Y., Rawlins, B. G. and Field, D. J.: Global soil organic carbon assessment. Glob Food Sec, 6, 9-16, https://doi.org/10.1016/j.gfs.2015.07.001, 2015.

Stockmann, U., Adams, M. A., Crawford, J. W., Field, D. J., Henakaarchchi, N., Jenkins, M., Minasny, B., McBratney, A. B., De Courcelles, V. d. R. and Singh, K.: The knowns, known unknowns and unknowns of sequestration of soil organic carbon. Agric Ecosyst Environ, 164, 80-99, https://doi.org/10.1016/j.agee.2012.10.001, 2013.

Terrer, C., Phillips, R. P., Hungate, B. A., Rosende, J., Pett-Ridge, J., Craig, M. E., van Groenigen, K. J., Keenan, T. F., Sulman, B. N., Stocker, B. D., Reich, P. B., Pellegrini, A. F. A., Pendall, E., Zhang, H., Evans, R. D., Carrillo, Y., Fisher, J. B., Van Sundert, K., Vicca, S. and Jackson, R. B.: A trade-off between plant and soil carbon storage under elevated CO2. Nature, 591, 599-603, https://doi.org/10.1038/s41586-021-03306-8, 2021.

Todd-Brown, K., Randerson, J., Hopkins, F., Arora, V., Hajima, T., Jones, C., Shevliakova, E., Tjiputra, J., Volodin, E. and Wu, T.: Changes in soil organic carbon storage predicted by Earth system models during the 21st century. Biogeosciences, 11, 2341-2356, https://doi.org/10.5194/bg-11-2341-2014, 2014.

Todd-Brown, K. E., Randerson, J. T., Post, W. M., Hoffman, F. M., Tarnocai, C., Schuur, E. A. and Allison, S. D.: Causes of variation in soil carbon simulations from CMIP5 Earth system models and comparison with observations. Biogeosciences, 10, 1717-1736, https://doi.org/10.5194/bg-10-1717-2013, 2013.

Viscarra Rossel, R. A., Webster, R., Bui, E. N. and Baldock, J. A.: Baseline map of organic carbon in Australian soil to support national carbon accounting and monitoring under climate change. Glob Change Biol, 20, 2953-2970, https://doi.org/10.1111/gcb.12569, 2014.

Viscarra Rossel, R. A., Chen, C., Grundy, M. J., Searle, R., Clifford, D. and Campbell, P. H.: The Australian three-dimensional soil grid: Australia's contribution to the GlobalSoilMap project. Soil Res, 53, 845-864, https://doi.org/10.1071/SR14366, 2015.

Viscarra Rossel, R. A., Lee, J., Behrens, T., Luo, Z., Baldock, J. and Richards, A.: Continental-scale soil carbon composition and vulnerability modulated by regional environmental controls. Nat Geosci, 12, 547-552, https://doi.org/10.1038/s41561-019-0373-z, 2019.

976 Viscarra Rossel, R. A., Webster, R., Zhang M., Shen, Z., Dixon, K., Wang, Y. P., Walden, L.:
977 How much organic carbon could the soil store? The carbon sequestration potential of
978 Australian soil. Glob Change Biol, 30, e17053, https://doi.org/10.1111/gcb.17053, 2023.
979 Wadoux, A. M. J., Román Dobarco, M., Malone, B., Minasny, B., McBratney, A. B. and Searle,
980 R.: Baseline high-resolution maps of organic carbon content in Australian soils. Sci Data, 10,
981 181, https://doi.org/10.1038/s41597-023-02056-8, 2023.
982 Walden, L., Serrano, O., Zhang, M., Shen, Z., Sippo, J. Z., Bennett, L. T., Maher, D. T.,
983 Lovelock, C. E., Macreadie, P. I. and Gorham, C.: Multi-scale mapping of Australia's
984 terrestrial and blue carbon stocks and their continental and bioregional drivers. Commun
985 Earth Environ, 4, 189, https://doi.org/10.1038/s43247-023-00838-x, 2023.
986 Wang, B., Waters, C., Orgill, S., Gray, J., Cowie, A., Clark, A. and Li Liu, D.: High resolution
987 mapping of soil organic carbon stocks using remote sensing variables in the semi-arid
988 rangelands of eastern Australia. Sci Total Environ, 630, 367-378,
989 https://doi.org/10.1016/j.scitotenv.2018.02.204, 2018a.
990 Wang, B., Gray, J. M., Waters, C. M., Anwar, M. R., Orgill, S. E., Cowie, A. L., Feng, P. and Li
991 Liu, D.: Modelling and mapping soil organic carbon stocks under future climate change in
992 south-eastern Australia. Geoderma, 405, 115442,
993 https://doi.org/10.1016/j.geoderma.2021.115442, 2022.
994 Wang, B., Waters, C., Orgill, S., Cowie, A., Clark, A., Li Liu, D., Simpson, M., McGowen, I.
995 and Sides, T.: Estimating soil organic carbon stocks using different modelling techniques in
996 the semi-arid rangelands of eastern Australia. Ecol Indic, 88, 425-438,
997 https://doi.org/10.1016/j.ecolind.2018.01.049, 2018b.
998 Wang, Y. P., Zhang, H., Ciais, P., Goll, D., Huang, Y., Wood, J. D., Ollinger, S. V., Tang, X. and
999 Prescher, A. K.: Microbial activity and root carbon inputs are more important than soil carbon
1000 diffusion in simulating soil carbon profiles. J Geophys Res Biogeosci, 126, e2020JG006205,
1001 https://doi.org/10.1029/2020JG006205, 2021.
1002 Wieder, W., Grandy, A., Kallenbach, C., Taylor, P. and Bonan, G.: Representing life in the Earth
1003 system with soil microbial functional traits in the MIMICS model. Geosci Model Dev, 8,
1004 1789-1808, https://doi.org/10.5194/gmd-8-1789-2015, 2015.
1005 Wiesmeier, M., Barthold, F., Spörlein, P., Geuß, U., Hangen, E., Reischl, A., Schilling, B.,
1006 Angst, G., von Lützow, M. and Kögel-Knabner, I.: Estimation of total organic carbon storage
1007 and its driving factors in soils of Bavaria (southeast Germany). Geoderma Regional, 1, 67-
1008 78, https://doi.org/10.1016/j.geodrs.2014.09.001, 2014.
1009 Wiesmeier, M., Urbanski, L., Hobley, E., Lang, B., von Lützow, M., Marin-Spiotta, E., van
1010 Wesemael, B., Rabot, E., Ließ, M. and Garcia-Franco, N.: Soil organic carbon storage as a
1011 key function of soils-A review of drivers and indicators at various scales. Geoderma, 333,
1012 149-162, https://doi.org/10.1016/j.geoderma.2018.07.026, 2019.
1013 Wynn, J. G., Bird, M. I., Vellen, L., Grand-Clement, E., Carter, J. and Berry, S. L.: Continental-
1014 scale measurement of the soil organic carbon pool with climatic, edaphic, and biotic controls.
1015 Global Biogeochem Cycles, 20, https://doi.org/10.1029/2005GB002576, 2006.
1016 Zhang, H., Goll, D. S., Wang, Y. P., Ciais, P., Wieder, W. R., Abramoff, R., Huang, Y., Guenet,
1017 B., Prescher, A. K. and Viscarra Rossel, R. A.: Microbial dynamics and soil physicochemical

properties explain large-scale variations in soil organic carbon. Glob Change Biol, 26, 2668-2685, https://doi.org/10.1111/gcb.14994, 2020.